



An online solid phase extraction method for the determination of ultratrace level phosphate in water with a high performance liquid chromatograph

Asaoka, Satoshi ; Kiso, Yoshiaki ; Oomori, Tsubasa ; Okamura, Hideo ; Yamada, Toshiro ; Nagai, Masahiro

(Citation)

Chemical Geology, 380:41-47

(Issue Date)

2014-07-25

(Resource Type)

journal article

(Version)

Accepted Manuscript

(Rights)

©2014.

This manuscript version is made available under the CC-BY-NC-ND 4.0 license
<http://creativecommons.org/licenses/by-nc-nd/4.0/>

(URL)

<https://hdl.handle.net/20.500.14094/90003340>



An Online Solid Phase Extraction Method for the Determination of Ultratrace Level
Phosphate in Water with a High Performance Liquid Chromatograph

Satoshi Asaoka¹, Yoshiaki Kiso², Tsubasa Oomori², Hideo Okamura¹, Toshiro Yamada³,
Masahiro Nagai⁴

¹ Research Center for Inland Seas, Kobe University, 5-1-1 Fukaeminamimachi,
Higashinada, Kobe, 658-0022 Japan

² Department of Environmental and Life Sciences, Toyohashi University of Technology,
Tempaku-cho, Toyohashi, 441-8580 Japan

³ Department of Civil Engineering, Faculty of Engineering, Gifu University, 1-1
Yanagido, Gifu 501-1193 Japan

⁴ Division of Human Environment, University of Human Environment,
Motojuku-cho, Okazaki, 444-3505 Japan

*Corresponding author

Satoshi Asaoka

Research Center for Inland Seas, Kobe University, 5-1-1 Fukaeminamimachi,
Higashinada, Kobe, 658-0022 Japan

Tel & Fax: +81-78-431-6357; Fax: +81-78-431-6357

E-mail: s-asaoka@maritime.kobe-u.ac.jp

Abstract

Phosphorous monitoring is important for eutrophication control in aquatic ecosystems, but ultratrace level concentrations may not be detected by conventional analytical methods. A method for measuring ultratrace level phosphate by online solid-phase extraction combined with HPLC was developed. A short column (50 mm) packed with octadecylsilane (ODS) was used for extraction of phosphoantimonymolybdenum blue and dodecyltrimethylammonium hydrophobic ion-pair complexes. The ion-pair complexes entrapped on the ODS column were eluted with CH₃CN/H₂O (35/65; flow rate, 1.0 ml min⁻¹) and monitored by an ultraviolet/visible spectrophotometer (λ =872 nm). Phosphate concentration was determined from the peak area of the ion pair. The limit of detection for orthophosphate was 0.15 $\mu\text{g PO}_4 \text{ l}^{-1}$ and the dynamic range was 0.15–100 $\mu\text{g PO}_4 \text{ l}^{-1}$. Although our method was susceptible to silicate interference, it could be corrected by a proposed interference correction equation.

Key words: Phosphate detection; Ultratrace detection; Ion pair;

dodecyltrimethylammonium ion

18 **Introduction**

19 Phosphorous is a limiting factor for primary production in aquatic ecosystems
20 because it is an essential nutrient for photosynthetic organisms. Agricultural runoff and
21 discharged wastewater contain excess phosphate (PO_4) that causes eutrophication in
22 closed water bodies, leading to undesirable growth of algae and toxic microbes such as
23 *Microcystis* (Lürling and Roessink, 2006), anaerobic conditions at the bottom of the
24 water bodies, and progression of organic pollution. Monitoring of ultratrace level
25 phosphate ($<2 \mu\text{g PO}_4 \text{ l}^{-1}$) including its distribution, transport, and chemical and
26 biological transformations, is an important aspect of eutrophication control and of
27 aquatic ecosystem modeling (Asaoka and Yamamoto, 2011; Arhonditsis and Brett,
28 2005; Luff and Moll, 2004; Tsiaras et al., 2014; Wei et al., 2004; Zhang and Chi, 2002).
29 Because of biological uptake, phosphate in surface water frequently goes undetected by
30 conventional analytical methods even in eutrophic water bodies (Wei et al., 2004). In
31 oligotrophic water bodies, phosphate is often present at concentrations less than $1 \mu\text{g l}^{-1}$,
32 below the limit of detection (LOD) of standard methods for measuring phosphate
33 concentration (APHA, 1999).

34 Phosphate analysis is commonly performed with a phosphoantimonymolybdenum
35 blue (PAMB) method (APHA, 1999) originally described by Murphy and Riley (1962).
36 In our proposed method, ammonium molybdate and potassium antimonyl tartrate react
37 in acid medium with orthophosphate to form a heteropoly acid, or phosphomolybdic
38 acid. The phosphomolybdic acid is reduced to intensely colored
39 phosphoantimonymolybdenum blue (PAMB) by ascorbic acid (APHA, 1999). Because
40 PAMB is an anionic species, it can form an ion pair with an organic cation such as
41 quaternary ammonium ions (Kiso et al., 2002).

42 Other methods for detecting trace phosphate are solvent extraction of PAMB;
43 complex formation of PAMB with cationic dyes such as rhodamine (Frank et al., 2006;

Nasu and Minami, 1989; Taniai et al., 2003), crystal violet (Fogg et al., 1977), or malachite green (Susanto et al., 1995a,; 1995b); and flow-injection analysis (APHA, 1999; Dinz et al. 2004; Estela and Cerdà, 2005; Mesquita et al., 2011; Ribeiro et al., 2013). Ultratrace levels of phosphate have also been detected by flow-injection analysis systems combined with PAMB-complex formation with a cationic dye (Li et al., 2005; Motomizu and Li, 2005; Susanto et al., 1995; Zhang and Chi, 2002; Yaqoob et al., 2004;). These systems required specially designed sophisticated instruments, and the reagent solutions were not stable (Li et al., 2005).

PAMB paired with quaternary ammonium salts can be extracted using a solid phase extraction technique (Liang et al, 2007; Ma et al., 2008). We developed a simple method for the detection of ultratrace phosphate by solid-phase extraction with HPLC. This method incorporates PAMB, an ionic species that forms hydrophobic ion-pair complexes with organic cation. We previously used PAMB and quaternary ammonium ion-pair formation to develop a spot test based on color-band formation in a mini column to detect PO_4 at concentrations of 3–18 mg l^{-1} (Kiso et al., 2002). In this study, an online solid-phase extraction unit equipped with an HPLC system was used to concentrate PAMB–quaternary ammonium ion pairs, which were detected by an ultraviolet/visible (UV/Vis) spectrophotometer after elution with an organic solvent.

In this study, the conditions for color development, ion-pair formation, extraction, and elution of the ion-pair were optimized to detect dissolved ultratrace level phosphate with a modified HPLC system.

2. Experimental

2.1 Reagents and solutions

All reagents were of analytical grade or the highest grade available. All reagent solutions were prepared with ultrapure water (18.2 $\text{M}\Omega \text{ cm}^{-1}$, Milli-Q Gradient A10;

Millipore, Billerica, MA, USA) and stored in polypropylene or poly(tetrafluoroethylene) bottles.

The stock solution of phosphate ($1000 \text{ mg PO}_4 \text{ l}^{-1}$) was prepared with KH_2PO_4 (Sigma-Aldrich, St. Louis, MO, USA), and the standard solutions were prepared by dilution of the stock solution at concentrations of $0.1\text{--}100 \text{ }\mu\text{g PO}_4 \text{ l}^{-1}$.

The mixed color reagent solution was prepared according to the US Standard Method (APHA, 1999) with reagents used as received from Nacalai Tesque (Kyoto, Japan): 5 ml of $2.743 \text{ g l}^{-1} \text{ K}(\text{SbO})\text{C}_4\text{H}_4\text{O}_6 \cdot 1/2\text{H}_2\text{O}$ solution, 15 ml of $40 \text{ g l}^{-1} (\text{NH}_4)_6\text{Mo}_7\text{O}_{24} \cdot 4\text{H}_2\text{O}$ solution, and 30 ml of 0.1 mol l^{-1} *L*-ascorbic acid solution were added to 50 ml of $2.5 \text{ mol l}^{-1} \text{ H}_2\text{SO}_4$ solution. Dodecyltrimethylammonium (DTMA) bromide was dissolved in methanol at 0.1% w/v. HPLC grade acetonitrile (CH_3CN) was used as the solvent for the solid-phase extraction.

Some researchers have reported the effects of interference ions such as Fe, Cu, Mn, Al, Zn, Pd and Ca on phosphate detection with using PAMB. Cu^{2+} caused a positive interference on phosphate determination over 10 mg l^{-1} (Galhardo et al., 2000). However, this concentration level is obviously low in natural and seawater samples. It was also reported that silica and arsenic reacted with ammonium molybdate (Murphy and Riley, 1962). Therefore, we tested the interference with co-ionic species for PO_4^{3-} detection using the following solutions: arsenate (As) (III) solution prepared with NaAsO_2 , As(V) solution with $\text{Na}_2\text{HAsO}_4 \cdot 7\text{H}_2\text{O}$, and Si solution with an analytical standard of Si for atomic absorbance.

2.2 Color development and ion-pair formation

To form PAMB, 2 ml of the mixed color reagent solution was added to 50 ml of the standard solution containing $10 \text{ }\mu\text{g PO}_4 \text{ l}^{-1}$. The reaction was conducted for 10 min at room temperature (approximately 20°C). Thereafter, 1.5 mL of DTMA solution was

added to the PAMB solution to form the PAMB-DTMA ion-pair complexes. This reaction was allowed to proceed under ultrasonication in an ice bath for 15 min.

2.3 Online solid-phase extraction-HPLC system

We combined an online solid-phase extraction unit with an HPLC system consisting of two pumps (880-PU and PU-2080 plus, JASCO), a sample injector (Rheodyne Model 7725i) equipped with a sample loop of 5 ml, a 6-way valve (Rheodyne Model 7000) equipped with a short column (4.6 mm i.d. × 50 mm long) packed with octadecylsilane (ODS; ULTRON VX-ODS, Shinwa Chemical Industry, Kyoto, Japan), and a UV/Vis detector (UV-2070 plus, JASCO). Chromatogram data were processed with JASCO-BORWIN/HSS-2000 programs. The system diagram and the operational procedure are shown in **Fig. 1**.

2.4 Online solid-phase extraction protocol

The solid-phase extraction of the PAMB-DTMA ion pairs was influenced by sample-loading and column-washing conditions, mobile-phase composition, and the flow rate of the mobile phase. On the basis of our examination of these variables, the following procedure was employed.

The solution containing PAMB-DTMA ion-pair complexes was injected into the sample loop (5 ml), then the solution was introduced into the ODS column with water at a 2.0 ml min⁻¹ flow rate by pump 1 (880-PU), followed by washing with 7 ml of water at a 2.0 ml min⁻¹ flow rate. The flow channel of the 6-way valve was changed and the entrapped ion-pair was eluted with CH₃CN/H₂O (35/65) at a 1.0 ml min⁻¹ flow rate by pump 2 (PU-2080 plus). Then the eluent was monitored by the UV/Vis detector (UV-2070 plus) at λ=872 nm. The 6-way valve was returned, and the ODS column was washed with water for approximately 3 min to condition the column.

2.5 Interference with co-ionic species

The solutions containing As(III), As(V), and Si were added to the standard solution containing $5 \mu\text{g PO}_4 \text{ l}^{-1}$ at the following concentrations: $5 \mu\text{g As(III) l}^{-1}$; 1, 3, and $5 \mu\text{g As(V) l}^{-1}$, and 5, 100, 2000, and $5000 \mu\text{g Si l}^{-1}$. These solutions were also employed for the analytical procedure described above.

2.6 Recommended online solid-phase extraction protocol to determine natural samples.

2.6.1 Reagents and solutions

The composition of the mixed color reagent solution was slightly modified to alleviate interference with silicate and diluent effect attributed to the addition of the mixed color reagent solution to samples. Five ml of $3.5 \text{ g l}^{-1} \text{ K(SbO)C}_4\text{H}_4\text{O}_6 \cdot 1/2\text{H}_2\text{O}$ solution, 15 ml of $52 \text{ g l}^{-1} (\text{NH}_4)_6\text{Mo}_7\text{O}_{24} \cdot 4\text{H}_2\text{O}$ solution, and 0.8 g of diluted *L*-ascorbic acid (1:9= *L*-ascorbic acid:NaCl) were added to 50 ml of $2.5 \text{ mol l}^{-1} \text{ H}_2\text{SO}_4$ solution. A 2.5 ml portion of this mixed color reagent solution was added to 25 mL samples, consistent with the final color reagent concentrations based on the US Standard Method (APHA, 1999). Dodecyltrimethylammonium (DTMA) bromide was dissolved in methanol at 0.1% w/v.

2.6.2 Color development and ion-pair formation

The normal protocol for the ion-pair formation was as follows: The mixed color reagent solution (2.5 mL) was added to 25 ml of the sample solution. The sample solution was kept at 50°C for 15 min to form PAMB. Thereafter, 0.75 ml of 0.1% w/v DTMA solution was added to the PAMB solution and the reaction mixture was agitated under ultrasonication in an ice bath for 15 min to form PAMB-DTMA complexes.

The optimum temperature for PAMB formation was examined under the following conditions: standard solution of $1 \text{ mg PO}_4 \text{ l}^{-1}$, temperature in the range of 25 to 70°C , the reaction time of 15 min, and absorbance measurement with a UV/Vis spectrophotometer (V-530; JASCO, Tokyo, Japan) using a 50 mm cell at $\lambda=880 \text{ nm}$.

The dosage of 0.1% w/v DTMA solution, which influences both the PAMB-DTMA ion-pair formation and efficiency of the online solid phase extraction, was examined by addition of 0-0.15 ml of 0.1% w/v DTMA solution to 25 mL of PAMB solution prepared with $10 \text{ }\mu\text{g PO}_4 \text{ l}^{-1}$ standard solution.

The reaction for PAMB-DTMA ion-pair complex formation was allowed to proceed under ultrasonication in an ice bath for 15 min. The peak area measurement of the PAMB-DTMA ion-pair complex was followed by the modified online solid phase extraction protocol to be described later (2.6.3).

To alleviate silicate interference on $\text{PO}_4 \text{ l}^{-1}$ measurement, the optimization of the final H_2SO_4 concentration in the PAMB solution was examined in the range of 0.28 to 0.56 g l^{-1} . Color development and PAMB-DTMA ion-pair complex formation were conducted as described earlier. The PAMB-DTMA complex was measured by the modified online solid phase extraction protocol to be described below (2.6.3).

2.6.3 Recommended online solid-phase extraction protocol

To improve efficiency of washing and conditioning of the ODS column, the mobile phase loading condition was slightly modified. The solution containing the PAMB-DTMA ion-pair complexes was injected into the sample loop (5 ml), then the solution was introduced into the ODS column with water at a 2.0 ml min^{-1} of flow rate by pump 1 (880-PU), followed by washing with 7 ml of water at 2.0 ml min^{-1} of flow rate. Then, the entrapped PAMB-DTMA ion-pair complexes were eluted using pump 2 (PU-2080 plus) by turning the 6-way valve, where the elution was conducted by gradient elution

mode when a gradient unit (LG-2080-02:JASCO) was located between a degassor (DG-2080-53:JASCO) and pump 2.

The mobile phase of CH₃CN/H₂O (30/70) was loaded at 1 mL min⁻¹ before eluting the PAMB-DTMA ion-pair (0-1.5 min). Thereafter the PAMB-DTMA ion-pair was eluted completely by CH₃CN/H₂O (35/65) at a flow rate of 1.0 mL min⁻¹ from 1.5 to 5.5 min. Thereafter, 100% of CH₃CN was loaded at a flow rate of 2 mL min⁻¹ for 5 min for column cleaning, and subsequently CH₃CN/H₂O (35/65) was loaded at 1.0 mL min⁻¹ flow rate for 3 min and pure water was loaded at 1.0 mL min⁻¹ for column conditioning. The eluent was monitored by the UV/Vis detector (UV-2070 plus) at $\lambda=872$ nm.

2.6.4 Effect of interference with silicate on PO₄ detection by the recommended online solid-phase extraction method

The effects of the interference with silicate and salinity on PO₄ analyses by the recommended online solid-phase extraction method was examined because silicate may compete with PAMB formation, and high salinity may influence the observed absorbance for common absorptiometry due to reflection.

Silicate interference was examined with silicate standard solution (0 to 20 mg Si l⁻¹) prepared by dilution of a 1000 mg l⁻¹ of a purchased silicate standard solution (analytical grade, Wako Pure Chemical). The prepared silicate solution was employed following the same protocol including the color development, ion-pair formation and online solid-phase extraction (see 2.6.2 and 2.6.3).

The effects of salinity were examined with the standard solutions of 0-10 $\mu\text{g PO}_4 \text{ l}^{-1}$ containing 3.5% NaCl. Phosphate detection was conducted using the same procedure described in 2.6.2 and 2.6.3.

2.6.5 Natural sample analyses with the recommended online solid-phase extraction

method

Two types of natural samples were collected from the Sea of Enshu and Kozenji-gawa River as shown in **Fig. 2**. Latitude and longitude of the sampling station of Kozenji-gawa river was 35°04'02.1"N and 136°04'01.8"E, respectively, and those of the Sea of Enshu are shown in **Table S1**. The Sea of Enshu is facing the Pacific Ocean along the coast of Shizuoka Prefecture, Japan. The surface seawater samples at 1 m depth and middle layer (sampling depth shown in **Table S1**) were collected by a Bandon water sampler on September 10th 2011. The collected samples were immediately filtered with a glass fiber filter (0.6 μm , Advantec) and transported to the laboratory in a container that was kept dark and cool. The samples were stored at -40°C before analyses.

Kozenji-gawa River is located in Shiga prefecture, Japan, flowing through an intermountain area surrounded by coniferous forests. The sampling station is located in headwater of Kozenji-gawa River within 20 ha catchment. The sampling was conducted every week from November 3rd, 2008 to April 26th, 2010. The collected stream water samples were filtered with a nuclepore filter (0.4 μm ; Whatman) and transported to the laboratory in a container that was kept dark and cool. The sample was stored at -40°C before analyses.

The stored samples (both sea water and river water samples) were analyzed by the same protocol for color development, ion-pair formation and online solid-phase extraction as described in 2.6.2 and 2.6.3.

3. Results and Discussion

3.1 Mobile phase for extraction

The mobile-phase compositions for elution of the retained ion pair on the ODS column were examined with 30%–100% aqueous CH_3CN . The chromatograms for 100 $\mu\text{g PO}_4 \text{ l}^{-1}$ standard solution showed two main peaks, peak A and peak B (**Fig. 3**). The

maximum absorbance of peak B was observed at 872 nm (**Fig. 4**), indicating that peak-B reflected the PAMB-DTMA ion-pair complex for which the spectra were obtained by the UV/Vis spectrophotometer (V-530). Peak A showed a broad spectrum that likely reflected the remaining reagents such as free DTMA.

Peak-B was separated from peak A at a CH₃CN content <40%. At CH₃CN=40%, however, a very small peak was detected just before peak B. At CH₃CN=30%, peak B broadened, and the peak intensity decreased markedly. Therefore, CH₃CN=35% was employed for optimum mobile-phase composition.

The area of peak B did not vary flow rates of 0.5 and 1.0 ml min⁻¹. Although the peak intensity at 0.5 ml min⁻¹ was lower (approximately 70%) than that at 1.0 ml min⁻¹, the symmetry factors of peak B were 1.23 and 1.54 for 0.5 and 1.0 ml min⁻¹, respectively. In the range of 1.0–2.0 ml min⁻¹, the peak area decreased with increased flow rate, owing to significant tailing of the peak. Therefore, a flow rate of 1.0 ml min⁻¹ was employed for the following experiments.

3.2 Sample loading and column washing

The flow rate for sample loading into the ODS column may have affected the extraction efficiency. Flow rate varied in the range of 1.0–4.0 ml min⁻¹ with the standard solution containing 10 µg PO₄ l⁻¹, but the areas of peak A and peak B were not influenced by the flow rate. On the basis of these results, we employed a flow rate of 2 ml min⁻¹ in the following experiments.

Because peak A was caused by the reagents remaining in the column, the column was washed with water to decrease peak A. The washing volume affected the chromatograms at a flow rate kept at 2 ml min⁻¹. The intensity of peak A decreased with increased washing volume, and peak A disappeared at washing volumes >6 ml (**Fig. 5**).

In our previous work on a spot test for color-band determination of phosphate (Kiso

et al., 2002), we employed benzylcetyldimethylammonium (BCDMA) as a quaternary ammonium ion. For the current method, however, when BCDMA was employed for the online extraction process, a large area of a blank sample was observed. Low water solubility of BCDMA may have prevented effective removal of the residual BCDMA by the washing process. When DTMA was used, the peak area of the blank sample decreased effectively; thus DTMA was a more suitable quaternary ammonium ion.

3.3 Interference

Because the molybdenum blue method is susceptible to interference from Si and As(V), we investigated the interfering effects of As(V), As(III), and Si for the standard solution of $5 \mu\text{g PO}_4 \text{ l}^{-1}$. The effects on the peak areas of these species are summarized in **Table 1**. No significant interference was seen from As(III) at $5 \mu\text{g As l}^{-1}$ or from Si at $<2000 \mu\text{g Si l}^{-1}$. Interference from As(V) gave error rates of +23.9% with $5 \mu\text{g As l}^{-1}$ and +8.5% at $3 \mu\text{g As l}^{-1}$ of As(V). This interference was attributable to formation of arsenoantimonymolybdenum blue–DTMA ion pairs that eluted at a retention time close to that of the PAMB-DTMA ion pairs (**Fig. 6a**). These different ion pairs were separated, however, under the mobile phase conditions of 0.5 ml min^{-1} (**Fig. 6b**). Considering that the intensity of peak B decreased at 0.5 ml min^{-1} , more efficient elution conditions such as a gradient elution mode may be necessary for simultaneous detection of PO_4^{3-} and As(V) at ultratrace levels.

3.4 Recommended online solid-phase extraction protocol to determine natural samples.

We hereby propose the recommended online solid-phase extraction protocol to detect ultra trace level phosphate in natural samples by slightly modifying the online solid-phase extraction protocol described above.

278

279 **3.4.1 Color development and ion-pair formation**

280 The optimum reaction temperature for color development was determined on the
281 basis of the intensity of absorbance at 880 nm. The absorbance of PAMB increased
282 asymptotically with increase of the reaction temperature and reached plateau level in the
283 range of over 50°C. Therefore, the color development reaction was conducted at 50°C in
284 the analysis that followed (**Fig. S1**).

285 The effect of DTMA dosage on the solid phase extraction of the PAMB-DTMA ion-
286 pair was evaluated under the following conditions: 0–1.5 ml of the DTMA solution and
287 25 ml of 10 µg PO₄ l⁻¹ PAMB solution. The peak area of the PAMB-DTMA ion-pair was
288 measured with the modified online solid-phase extraction protocol. The peak area
289 reached the maximum when 0.75 mL of the DTMA solution was added to 25 ml of the
290 PAMB solution (**Fig. S2**). The peak area decreased rapidly when the DTMA solution
291 dosage increased more than 1 ml, and this was caused by the precipitation of ion-pair
292 complex.

293 Silicate reacted with ammonium molybdate (Murphy and Riley, 1962). This reaction
294 is influenced by H₂SO₄ concentration. Therefore, the final concentration of H₂SO₄ in the
295 PAMB solution was changed into the range of 0.28 to 0.56 g l⁻¹ (**Fig. 7**). In the case
296 when H₂SO₄ concentration was more than 0.42 g l⁻¹, both the peak areas of PO₄ (10 µg
297 PO₄ l⁻¹) solution and PO₄ (10 µg PO₄ l⁻¹) + silicate mixed solution (10 mg Si l⁻¹)
298 decreased. When lower than 0.35 g l⁻¹ H₂SO₄ concentration, however, the peak area of
299 the PO₄ + silicate mixed solution was obviously larger than that of the PO₄ solution. The
300 interference with silicate was unavoidable, therefore 0.35 g l⁻¹ of the final concentration
301 of H₂SO₄ in the PAMB solution was employed in this work.

302

303 **3.4.2 Calibration curve with the recommended online solid-phase extraction method**

The calibration curve for phosphate ($0\text{--}100\ \mu\text{g PO}_4\ \text{l}^{-1}$) is shown in **Fig. 8**. The reproducibility of the proposed method was examined for the ultratrace level standard solutions. The average peak areas ($0.2\text{--}100\ \mu\text{g PO}_4\ \text{l}^{-1}$) and the RSDs ($n=3$) are 0.64–8.26%. Based on the RSD of the blank sample, the LOD (S/N ratio=3) was evaluated to be $0.15\text{-}\mu\text{g PO}_4\ \text{l}^{-1}$ ($0.05\ \mu\text{g P l}^{-1}$). The LOD obtained in this study is similar to the lowest levels reported for all other methods (Ma et al., 2008; Li, et al., 2005; Liang et al, 2007; Susanto et al., 1995b; Wu and Ruzicka, 2001; Yaqoob, et al., 2004; Zhang and Chi, 2002).

The dynamic range of this recommended method was $0.15\text{--}100\text{-}\mu\text{g PO}_4\ \text{l}^{-1}$ ($0.05\text{--}33\text{-}\mu\text{g P l}^{-1}$) and is extremely wide in comparison with the other analytical methods for ultratrace level phosphate (Frank et al., 2006; Li et al., 2005; Mesquita et al., 2011; Susanto et al., 1995; Wu and Ruzicka, 2001; Yaqoob, et al., 2004; Zhang and Chi, 2002).

Although manual sample preparation processes were required for the color development and the ion-pair formation, the proposed method has the following advantages: when sample absorbance was lower than the detection limit in conventional PAMB methods, the PAMB solutions can be analyzed using the proposed method only after the addition of the DTMA solution.

3.4.3 Effect of salinity and silicate on PO_4 analyses with the recommended online solid-phase extraction method

The effect of salinity on PO_4 detection using the modified online solid-phase extraction method was examined on the basis of the calibration curves for the PO_4 ($0\text{--}10\ \mu\text{g PO}_4\ \text{l}^{-1}$) standard solutions with and without distilled ion exchange water and 3.5% NaCl. The difference between both calibration curves was very small as shown in **Fig. S3**: the differences of the peak area were in the range of -1.2 to 1.7% . The results

revealed that the effect of salt concentration in sea water samples can be negligible.

The calibration curve for silicate (0-20 mg l⁻¹) obtained by the modified online solid-phase extraction method is shown in **Fig. S4**. Silicate caused positive error in the quantification of trace level phosphate, although the effect of silicate can be negligible for phosphate detection in the concentration range measured by common absorptiometry. When both peak areas for phosphate and silicate are measured under same conditions, the effect of silicate on phosphate detection can be evaluated as a correction equation. Figure 9 shows the correction equation. For example, the peak area for 5 mg l⁻¹ silicate corresponds to that for 2.1 µg PO₄ l⁻¹. Therefore, when PO₄ concentration in samples was much lower than that of silicate, PO₄ concentration should be corrected by eliminating interference with silicate.

3.4.4 Determination of PO₄ concentration in natural samples with the recommended online solid-phase extraction method

The concentrations of PO₄ in surface seawater collected from the Pacific Ocean was 1.35 to 8.42 µg PO₄ l⁻¹ and 1.39 to 8.50 µg PO₄ l⁻¹ under rising tide and ebbing tide conditions, respectively (**Table 2**). The phosphate concentrations of the middle layer were 1.25 to 3.74 µg PO₄ l⁻¹ (rising tide) and 0.41 to 1.98 µg PO₄ l⁻¹ (ebbing tide). To verify the effect of salinity on the detected PO₄ in seawater, the standard addition method was conducted for the sample of the middle layer (rising tide) at St. 7 (**Fig. S5**). The salinity of the sample was 3.4‰ and the detected PO₄ concentration was 1.71 µg PO₄ l⁻¹. On the other hand, the PO₄ concentration by the standard addition method was 1.29 µg PO₄ l⁻¹. Both values are quite similar, and it was revealed that the recommended method was not influenced by salinity.

The Kozenji river samples were measured using the recommended online solid-phase extraction method (**Fig. 10**). Observed PO₄ concentration was overestimated because

the samples contained silicate in the range of 6.04 to 9.54 mg l⁻¹. Therefore, PO₄ concentration was corrected by using the interference correction equation shown in **Fig. 9**. The corrected PO₄ concentrations in Kozenji river were in the range from <0.15 to 8.92 µg PO₄ l⁻¹. The recommended online solid-phase extraction method could determine ultratrace or trace level PO₄ effectively compared to the conventional method.

4. Conclusion

This study demonstrated the effectiveness of an online solid-phase extraction method for the detection of ultratrace level phosphate. Under the recommended conditions, the LOD was 0.15 µg PO₄ l⁻¹ with the dynamic range of 0.15–100 µg PO₄ l⁻¹. The proposed method involves manual procedures for color development and ion-pair formation, but requires only an HPLC system. In addition, it was indicated that the proposed method was not influenced by salinity and that silicate interference can be eliminated by using the interference correction equation.

Acknowledgement

This work was financially supported by the 21st Century Center of Excellence (COE) Program Ecological Engineering for Homeostatic Human Activities, sponsored by the Ministry of Education, Culture, Sports, Science and Technology of Japan. We also thank Professor Dr. Shinichi Aoki.

References

- Asaoka, S., Yamamoto, T., 2011. Phosphorus mass balance in a highly eutrophic semi-enclosed inlet near a big metropolis: A small Inlet can contribute towards particulate organic matter production. *Mar. Pollut. Bull.* 63, 237-242.
- American Public Health Association (APHA), 1999. Standard method for examination of water and wastewater. 20th Edition. Washington, DC. 4500P-F.
- Arhonditsis, G.B., Brett M.T., 2005. Eutrophication model for Lake Washington (USA): Part II: model calibration and system dynamics analysis. *Ecol. Model.* 187, 179-200.
- Dinz, M.C.T., Filho, O.F., De Aquino, E.V., Rohwedder, J.J.R., 2004. Determination of phosphate in natural water employing a monosegmented flow system with simultaneous multiple injection. *Talanta*. 62, 469-475.
- Estela, J.M., Cerdà, V., 2005. Flow analysis techniques for phosphorus: an overview. *Talanta*. 66, 307-331.
- Fogg, A.G., Soleymanloo, S., Burns, D.T., 1977. The spectrophotometric determination of inorganic phosphate in biological systems with crystal violet. *Anal. Chim. Acta*. 88, 197-200.
- Frank, C. Schroeder, F., Ebinghaus, R., Ruck, W., 2006. Using sequential injection analysis for fast determination of phosphate in coastal waters. *Talanta* 70, 513-517.
- Galhardo, C. X., Masini J. C., 2000. Spectrophotometric determination of phosphate and silicate by sequential injection using molybdenum blue chemistry. *Anal. Chim. Acta* 417, 191-200.
- Kiso, Y., Kuzawa, K., Saito, Y., Yamada, T., Nagai, M., Jung, Y.-J., Min, K.-S., 2002. A spot test for aqueous phosphate by color band formation. *Anal. Bioanal. Chem.*, 374, 1212-1217.
- Li, Z., Oshima, M., Sabarudin, A., Motomizu, S., 2005. Trace and ultratrace analysis of

purified water samples and hydrogen peroxide solutions for phosphorous by flow-injection method. Anal. Sci. 21,263-268.

Liang, Y., Yuan, D., Li, Q., Lin, Q. 2007. Flow injection analysis of nanomolar level orthophosphate in seawater with solid phase enrichment and colorimetric detection. Mar. Chem., 103, 122-130.

Luff, R., Moll, A., 2004. Seasonal dynamics of the North Sea sediments using a three-dimensional coupled sediment-water model system. Cont. Shelf Res. 24, 1099-1127.

Lürling, M., Roessink, I., 2006. On the way to cyanobacterial blooms: Impact of the herbicide metribuzin on the competition between a green alga (*Scenedesmus*) and a cyanobacterium (*Microcystis*). Chemosphere. 65, 618-626.

Ma, J., Yuan, D., Liang, Y., Dai, M., 2008. A modified analytical method for the shipboard determination of nanomolar concentrations of orthophosphate in seawater. J. Oceanogr., 64, 443-449.

Mesquita, R.B.R., Ferreira, M.T.S.O.B., Tóth, I.V., Bordalo, A.A., McKelvie, I. D., Rangel, A.O.S.S., 2011. Development of a flow method for the determination of phosphate in estuarine and freshwaters-Comparison of flow cells in spectrophotometric sequential injection analysis. Anal. Chim. Acta 701, 15-22.

Motomizu S., Li, Z.H., 2005. Trace and ultratrace analysis methods for the determination of phosphorus by flow-injection techniques. Talanta 66, 332-340.

Murphy, J. Riley, J. P., 1962. A modified single solution method for the determination of phosphate in natural waters. Anal. Chem. Acta. 27, 31-36.

Nasu, T., Minami, H., 1989. Flotation-spectrofluorimetric determination of phosphate in natural water using Rhodamine B as an ion-pair reagent. Analyst. 114, 955-958.

Ribeiro, M.F.T., Couto, C.M.C.M., Conceição, P.M.M., Santos, J.L.M., 2013. An automated multi-pumping pulsed flow system with spectrophotometric detection for the determination of phosphate in natural waters. Anal. Lett. 46, 1769-1778.

429 Susanto, J.P., Oshima, M., Motomizu, S., Mikasa, H., Hori, Y., 1995a. Adsorption-
430 concentration of ion associate formed between molybdosilicate and malachite green
431 on a miniature filter: its application to trace and ultratrace determination of silicon.
432 *Analyst.* 120, 2605-2611.

433 Susanto, J.P., Oshima, M., Motomizu, S., Mikasa, H., Hori, Y., 1995b. Determination of
434 micro amounts of phosphorous with Malachite green using a filtration-dissolution
435 preconcentration method and flow injection-spectrophotometric detection. *Analyst.*
436 120, 187-191.

437 Taniai, T., Sukegawa, M., Sakuragawa, A., Uzawa, A., 2003. On-line preconcentration
438 of phosphate onto molybdate form anion exchange column. *Talanta*, 61, 905-912.

439 Tsiaras, K.P., Petihakis, G., Kourafalou, V. H., Triantafyllou, G., 2014. Impact of the
440 river nutrient load variability on the North Aegean ecosystem functioning over the
441 last decades. *J. Sea Res.* 86, 97-109.

442 Wei, H., Sun, J., Moll, A., Zhao, L., 2004. Phytoplankton dynamics in the Bohai Sea-
443 observations and modeling. *J. Mar. Syst.* 44, 233-251.

444 Wu, C.H., Ruzicka, J., 2001. Micro sequential injection: environmental monitoring of
445 nitrogen and phosphate in water using a “Lab-on-Valve” system furnished with a
446 microcolumn. *Analyst.* 126, 1947-1952.

447 Yaqoob, M., Nabi, A., Worsfold, P., 2004. Determination of nanomolar concentrations
448 of phosphate in freshwaters using flow injection with luminol chemiluminescence
449 detection. *Anal. Chim. Acta.* 510, 213-218.

450 Zhang, J.Z., Chi, J., 2002. Automated analysis of nanomolar concentrations of
451 phosphate in natural waters with liquid waveguide. *Environ. Sci. Technol.* 36, 1048-
452 1053.

Figure captions

Fig. 1 Diagram of the online extraction system and operational procedure

Fig. 2 Sampling stations on the Sea of Enshu and Kozenji-gawa River

Fig. 3 Effect of the mobile phase composition on chromatograms

Sample: $100\ \mu\text{g PO}_4\text{ l}^{-1}$; Sample loading rate: $2.0\ \text{ml min}^{-1}$; Washing volume: 5 ml ;

Flow rate of the mobile-phase: $1.0\ \text{ml min}^{-1}$

Fig. 4 Absorption spectrum of peak-A and peak-B

Fig. 5 Effect of the volume for column washing on the chromatogram

Sample: $10\ \mu\text{g-PO}_4\text{ l}^{-1}$; Sample loading rate: $2.0\ \text{ml min}^{-1}$; mobile phase:

$\text{CH}_3\text{CN}/\text{H}_2\text{O}=35/65$: flow rate of the mobile phase: $1.0\ \text{ml min}^{-1}$

Fig. 6 Separation of PO_4^{3-} and As(V)

Phosphate concentration: $5\ \mu\text{g PO}_4\text{ l}^{-1}$; Arsenate concentration: $5\ \mu\text{g-As(III) l}^{-1}$

(a) Mobile-phase: $\text{CH}_3\text{CN}/\text{H}_2\text{O}=35/65$ at $1.0\ \text{ml min}^{-1}$; $\lambda=872\ \text{nm}$

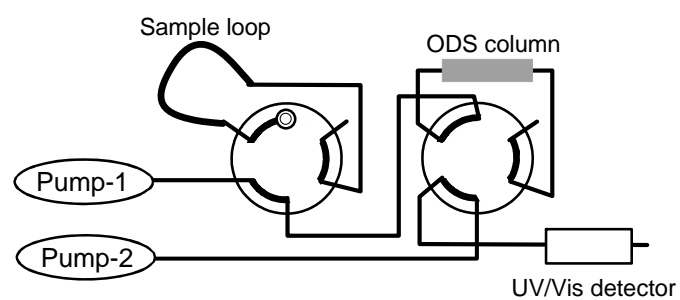
(b) Mobile-phase: CH_3CN (100%) at $0.5\ \text{ml min}^{-1}$; $\lambda=872\ \text{nm}$

Fig.7 Effect of H_2SO_4 final concentration in PAMB solution on the peak area of PO_4 or PO_4 and Si mixed solution

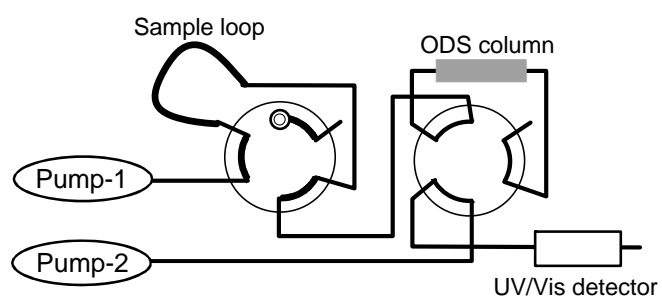
Fig. 8 Calibration curves for PO_4 using modified online solid phase extraction method.

Fig. 9 Compensation equation calculated from the peak areas of silicate and trace level phosphate

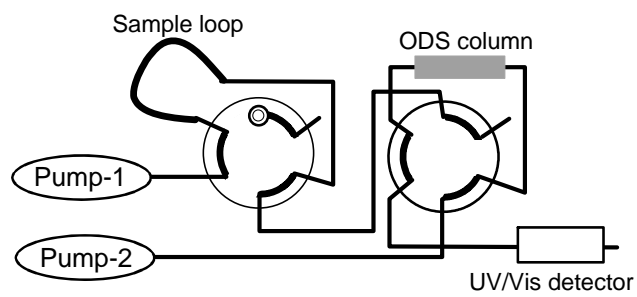
Fig. 10 Concentration of PO_4 in Kozenji-gawa River water



(A) Sample injection and column conditioning



(B) Sample loading to ODS column



(C) Elution and detection

Fig. 1

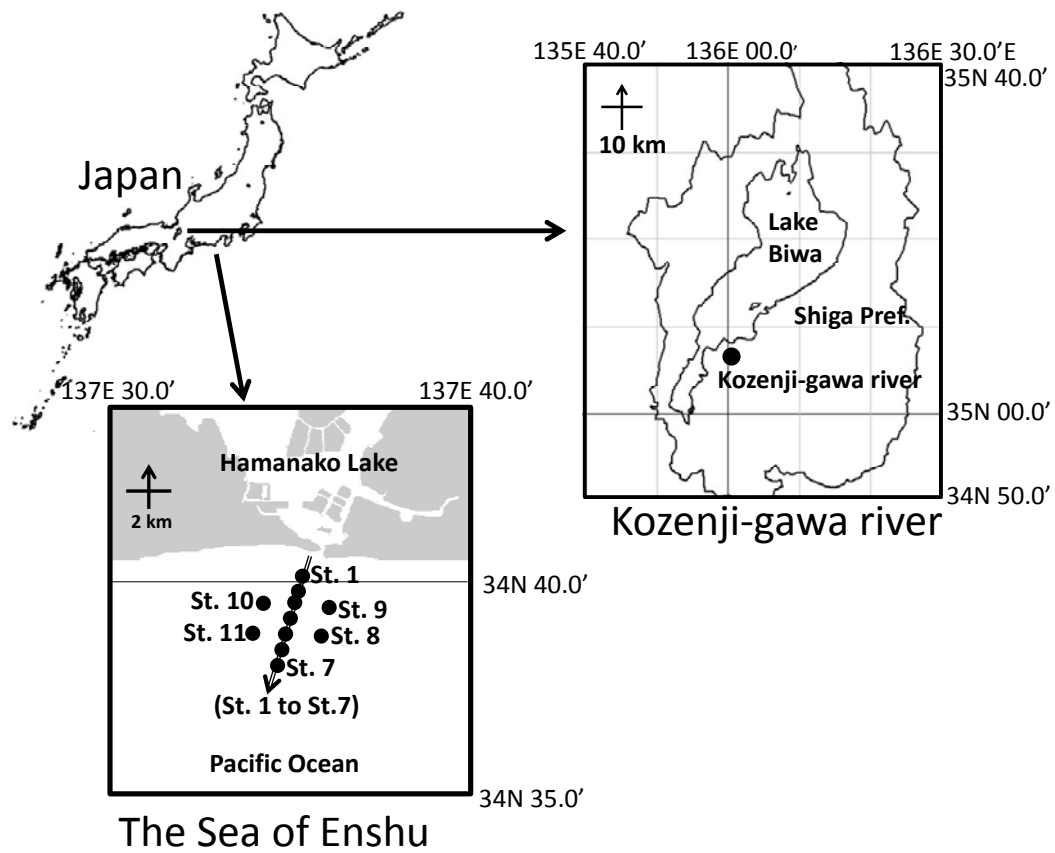


Fig. 2

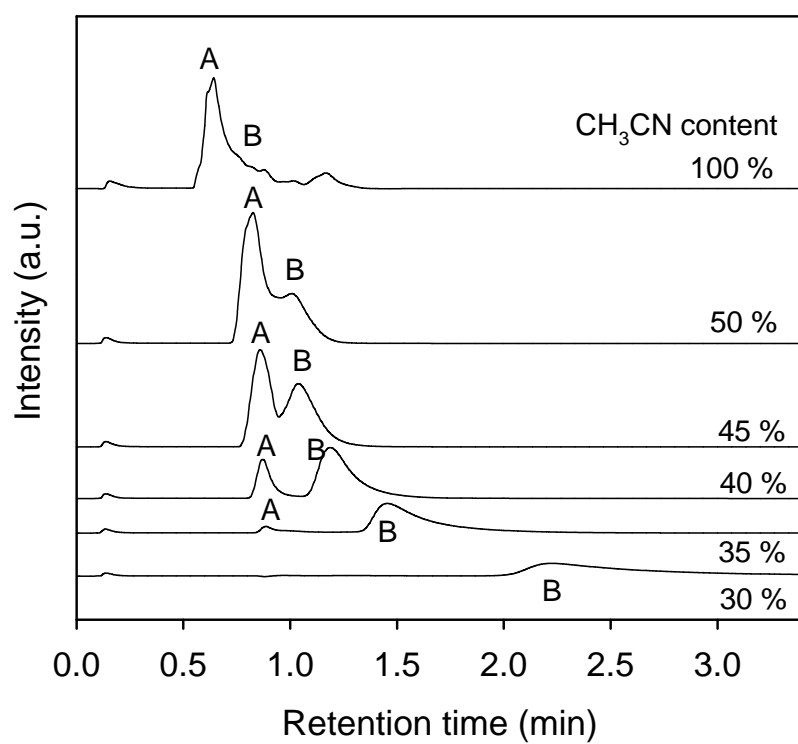


Fig. 3

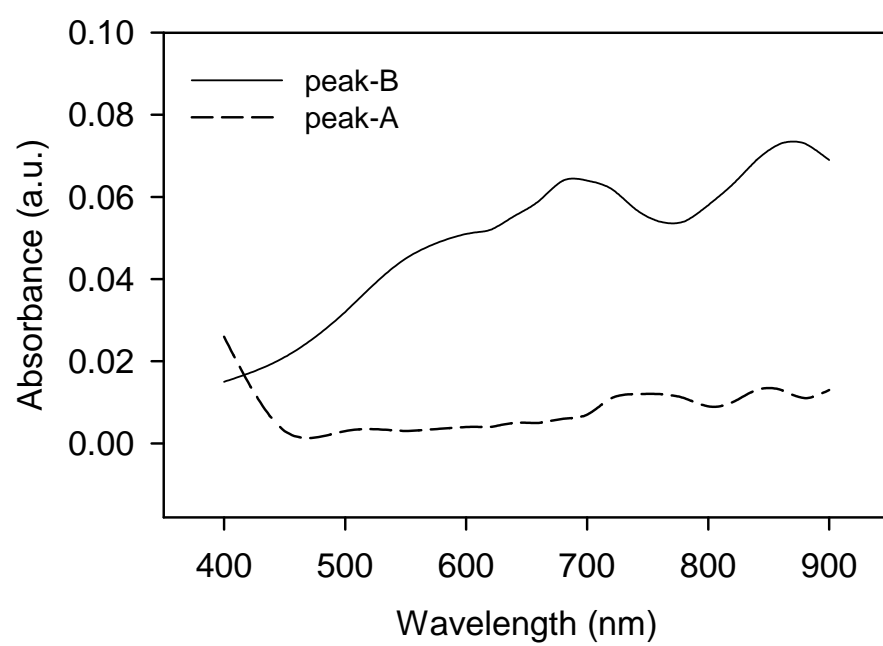


Fig. 4

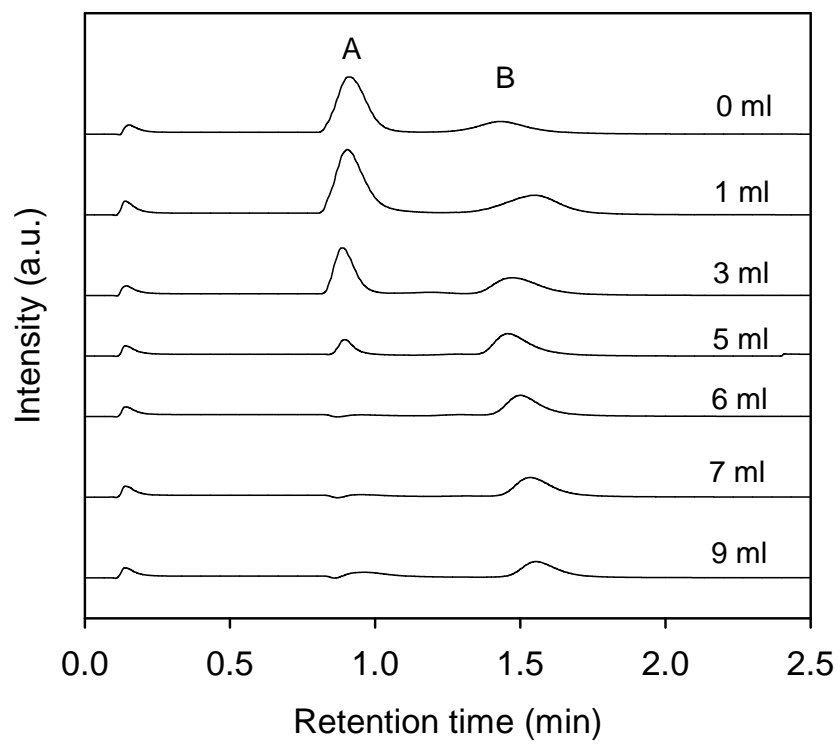


Fig. 5

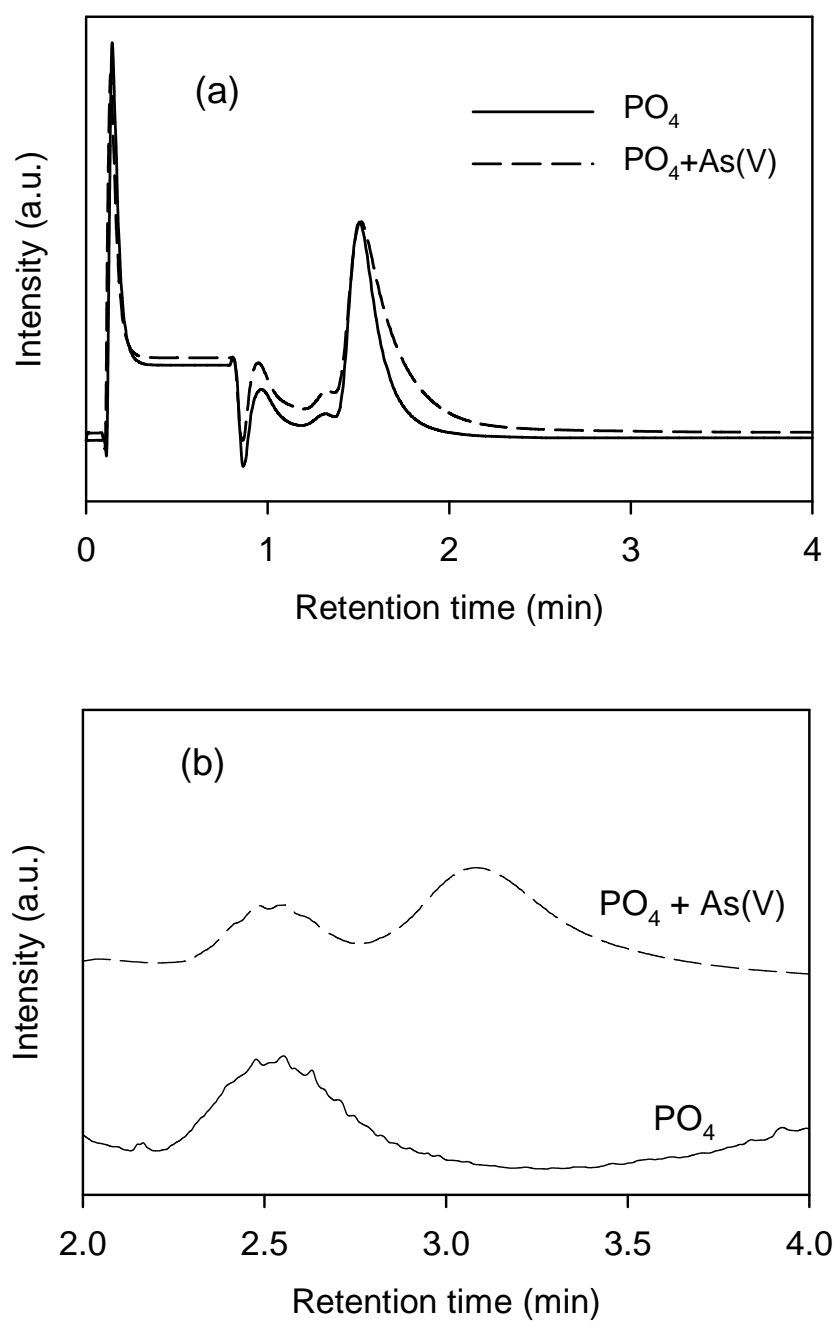


Fig. 6

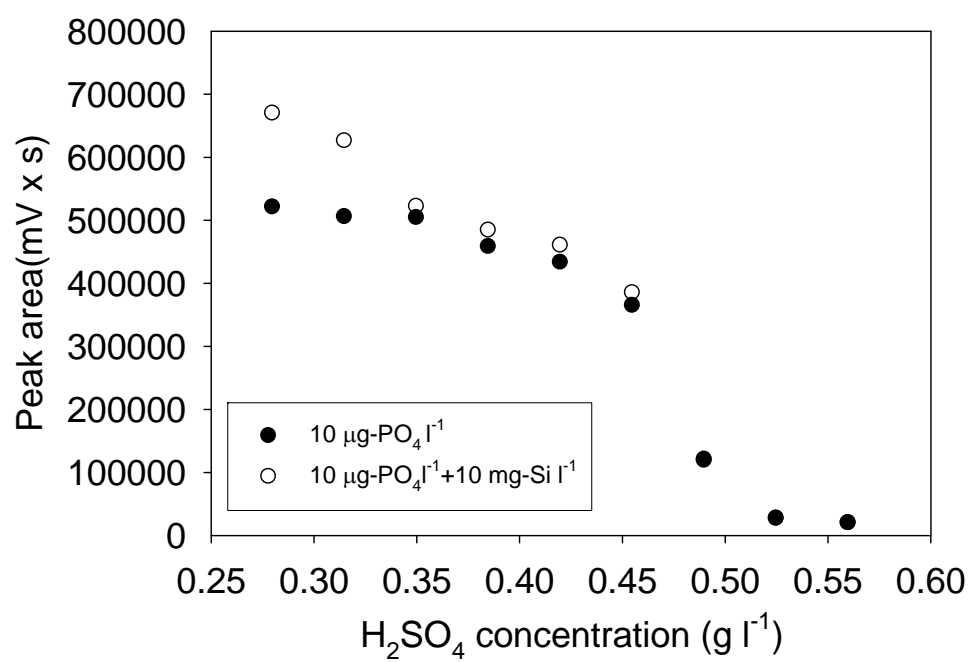


Fig.7

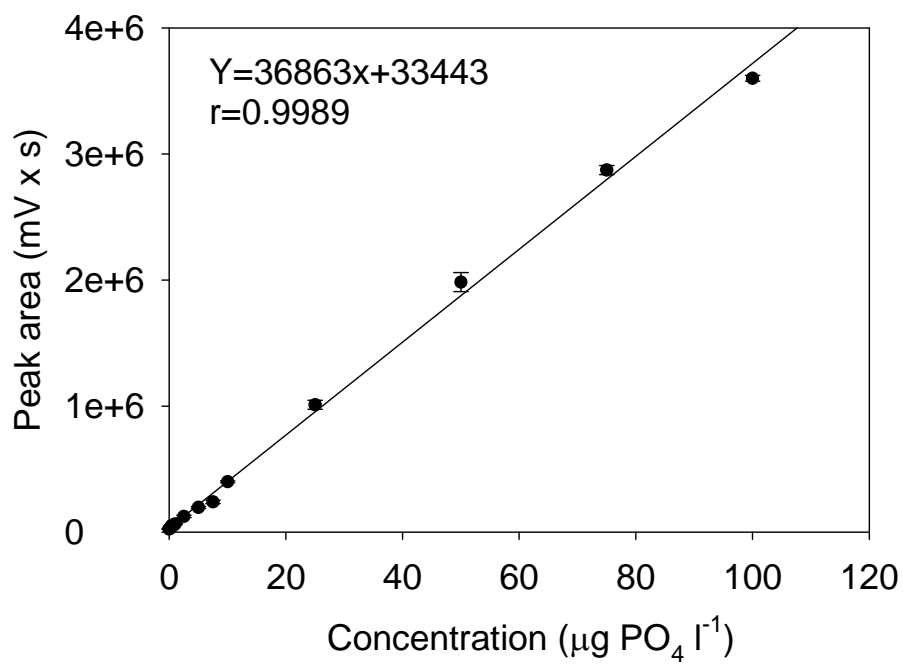


Fig. 8

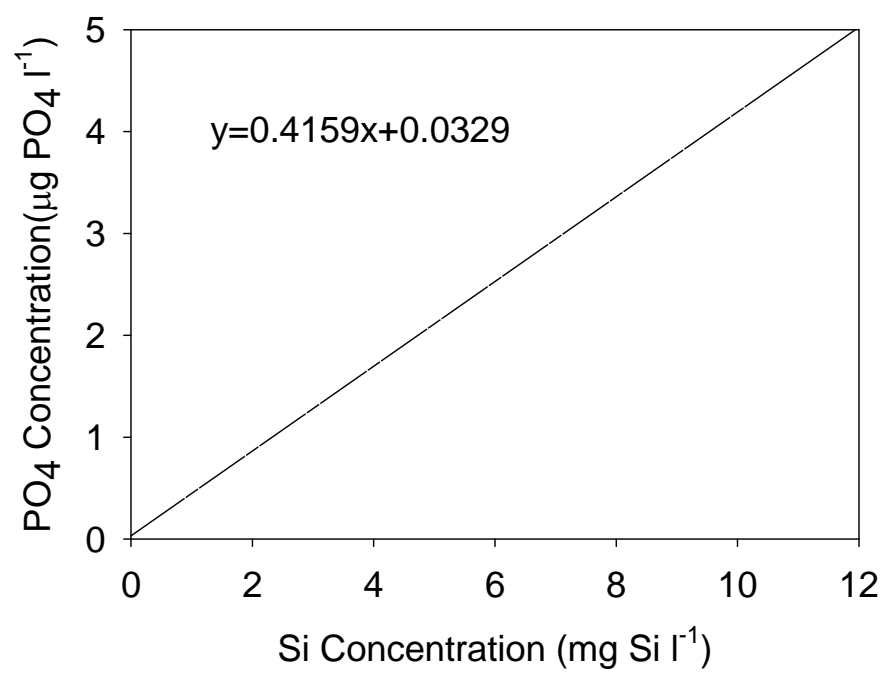


Fig. 9

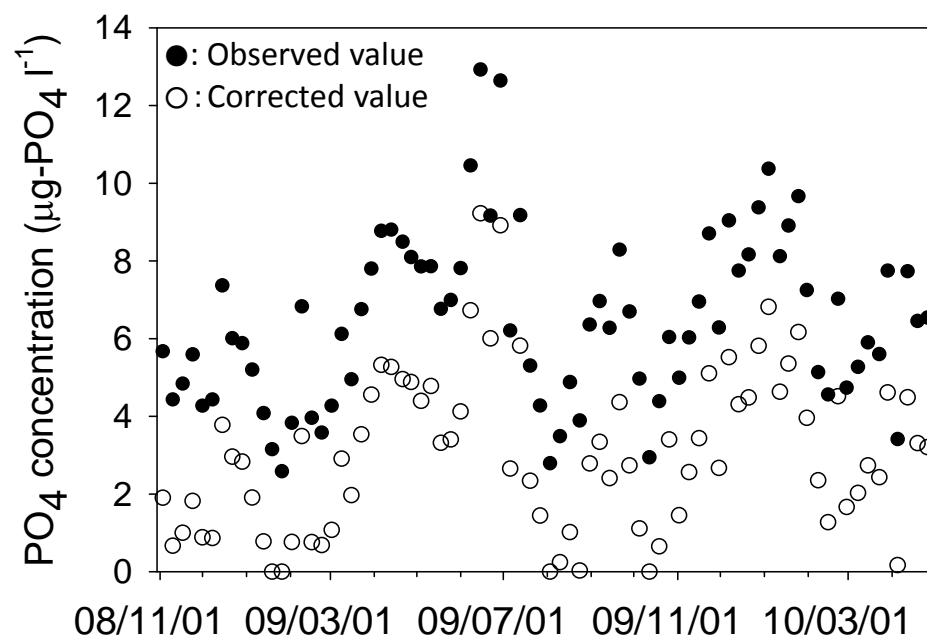


Fig. 10

Table 1 Interference from chemical species on phosphate detection

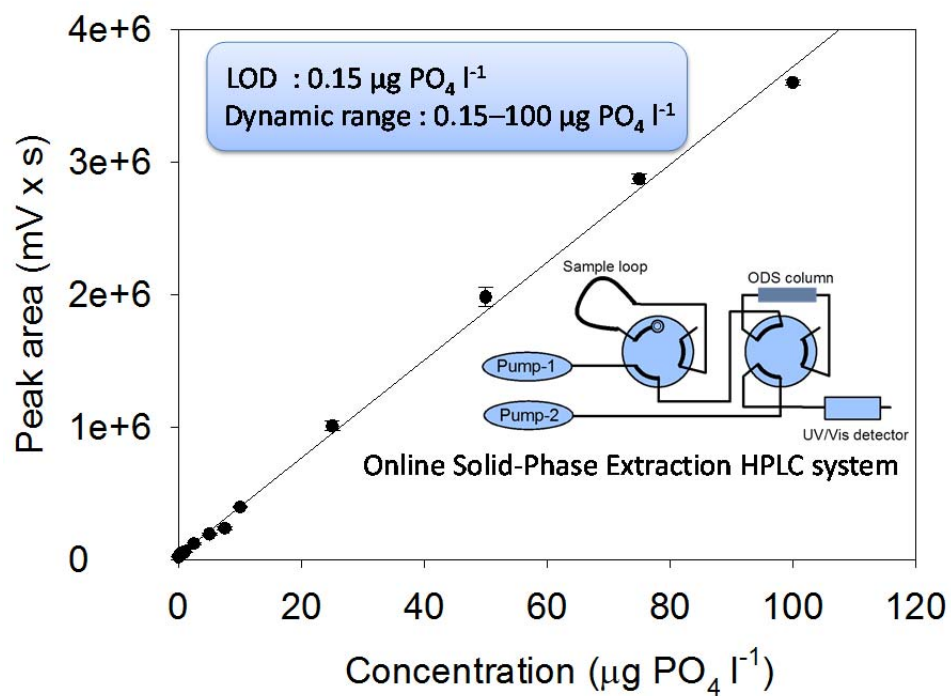
Phosphate concentration: 5 $\mu\text{g PO}_4 \text{ l}^{-1}$

Species	Concentration	Error (%)
As(V)	1 $\mu\text{g l}^{-1}$	+2.7
	3 $\mu\text{g l}^{-1}$	+8.5
	5 $\mu\text{g l}^{-1}$	+23.9
As (III)	5 $\mu\text{g l}^{-1}$	+3.6
Si	5 $\mu\text{g l}^{-1}$	-1.5
	100 $\mu\text{g l}^{-1}$	+1.1
	2000 $\mu\text{g l}^{-1}$	+10.3
	5000 $\mu\text{g l}^{-1}$	+27.1

Table 2 Concentration of PO_4 in seawater collected from the Sea of Eshu ($\mu\text{g PO}_4 \text{ l}^{-1}$)

Station	Surface later		Middle layer	
	Rising tide	Ebbing tide	Rising tide	Ebbing tide
St.1	2.51	3.22	2.71	0.51
St.2	5.68	1.46	2.59	0.41
St.3	5.59	8.5	3.15	0.47
St.4	4.45	4.84	1.37	0.48
St.5	3.62	2.17	2.7	0.8
St.6	3.43	3.23	1.25	0.78
St.7	8.42	1.39	1.71	0.83
St.8	5.95	1.73	3.74	0.82
St.9	4.05	3.15	3.02	1.98
St.10	1.35	2.05	2.46	1.07
St.11	1.71	1.66	1.44	0.92

Graphical Abstract



Supplemental material

An Online Solid Phase Extraction Method for the Determination of Ultratrace Level
Phosphate in Water with a High Performance Liquid Chromatograph

Satoshi Asaoka¹, Yoshiaki Kiso², Tsubasa Oomori², Hideo Okamura¹, Toshiro Yamada³,
Masahiro Nagai⁴

¹ Research Center for Inland Seas, Kobe University, 5-1-1 Fukaeminamimachi,
Higashinada, Kobe, 658-0022 Japan

² Department of Environmental and Life Sciences, Toyohashi University of Technology,
Tempaku-cho, Toyohashi, 441-8580 Japan

³ Department of Civil Engineering, Faculty of Engineering, Gifu University, 1-1
Yanagido, Gifu 501-1193 Japan

⁴ Division of Human Environment, University of Human Environment
Motojuku-cho, Okazaki, 444-3505 Japan

*Corresponding author

Satoshi Asaoka

Research Center for Inland Seas, Kobe University, 5-1-1 Fukaeminamimachi,
Higashinada, Kobe, 658-0022 Japan

Tel & Fax: +81-78-431-6357; Fax: +81-78-431-6357

E-mail: s-asaoka@maritime.kobe-u.ac.jp

Table S1 Latitude and Longitude of sampling stations in the Sea of Enshu

Stations	Latitude	Longitude	Sampling depth (m)
St.1	34°40'14"N	137°35'42"E	1 and 5
St.2	34°40'01"N	137°35'36"E	1 and 10
St.3	34°39'45"N	137°35'29"E	1 and 15
St.4	34°39'22"N	137°35'18"E	1 and 15
St.5	34°38'59"N	137°35'08"E	1 and 15
St.6	34°38'23"N	137°34'51"E	1 and 15
St.7	34°37'31"N	137°34'27"E	1 and 15
St.8	34°38'59"N	137°36'15"E	1 and 15
St.9	34°39'45"N	137°36'33"E	1 and 15
St.10	34°39'45"N	137°34'23"E	1 and 15
St.11	34°38'59"N	137°34'01"E	1 and 15

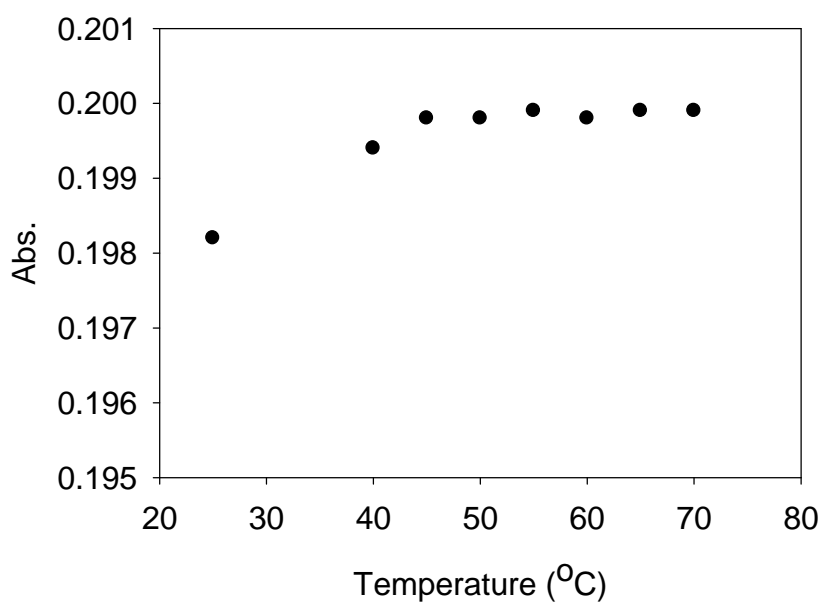


Fig. S1 Effect of reaction temperature on PAMB absorbance

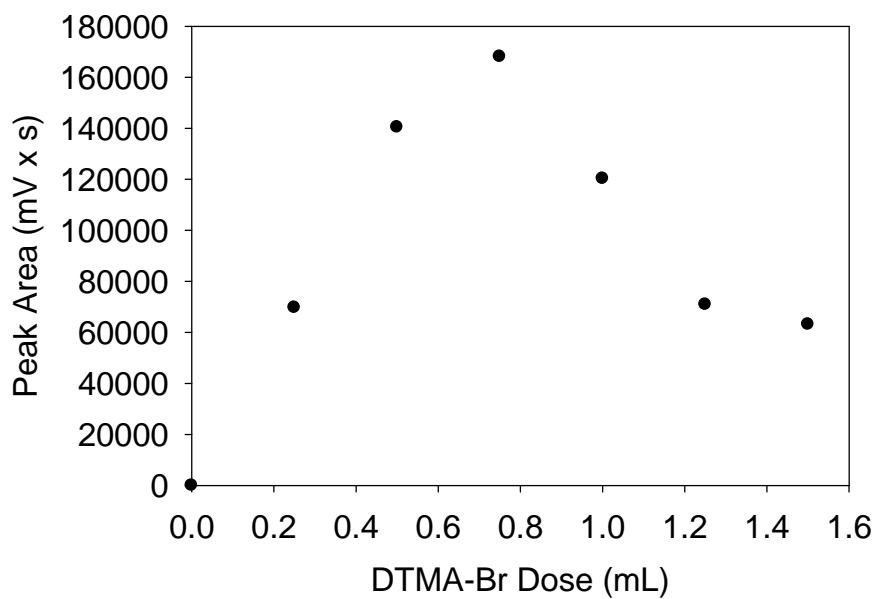


Fig. S2 Effect of DTMA dose on the peak area of the PAMB-DTMA ion-pair complexes using the modified online solid phase method

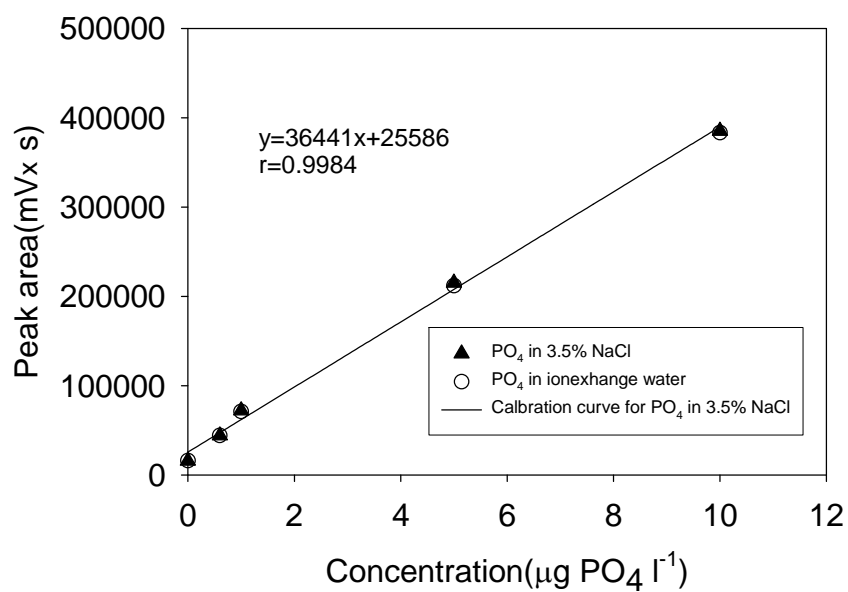


Fig. S3 Calibration curve for PO₄ in ion exchange water or 3.5% NaCl solution

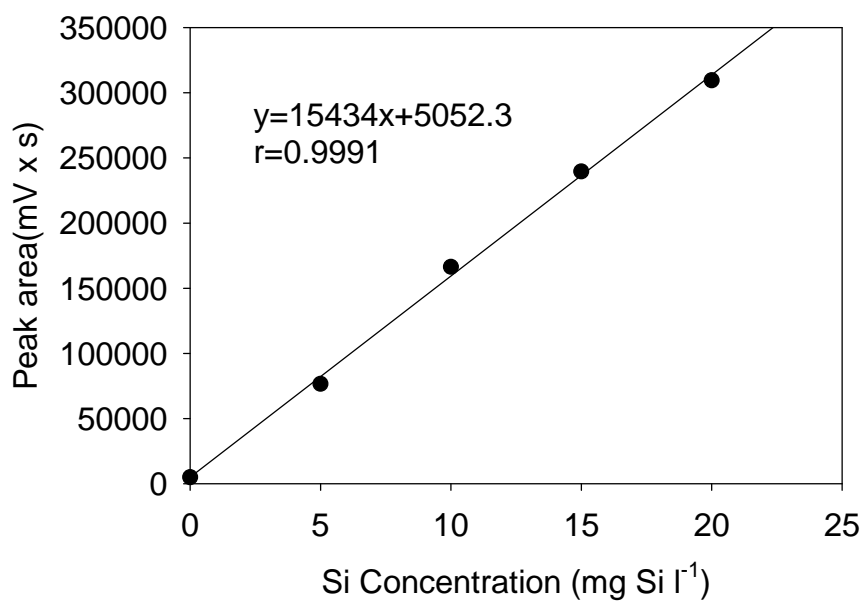


Fig. S4 Calibration curves for silicate obtained by the modified online solid phase extraction method

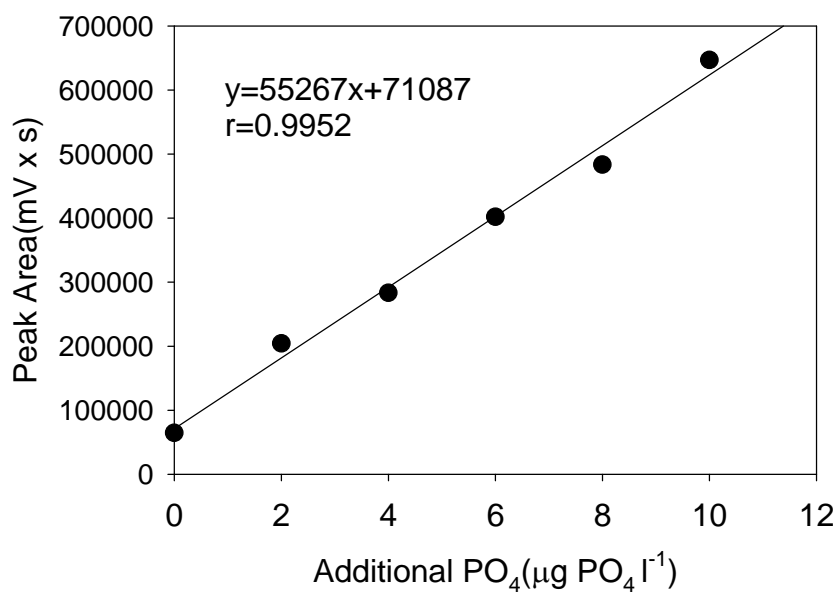


Fig. S5 Concentration of PO₄ in seawater collected from station 7 in the Sea of Enshu determined by standard addition method using the modified solid phase extraction method